

RESEARCH

Open Access



The application of dual-phase enhanced CT scan in distinguishing adrenal ganglioneuromas from adrenal lipid-poor adenomas

Huajun Yu^{1†}, Jian Wang^{2†}, Zhongfeng Niu³ and Meihua Shao^{2*} 

Abstract

Background The utility of dual-phase enhanced computerized tomography (CT) scan in distinguishing adrenal ganglioneuromas from lipid-poor adenomas has not been reported. We aimed to retrospectively compare dual-phase enhanced CT findings which were helpful in distinguishing adrenal ganglioneuromas from adrenal lipid-poor adenomas.

Methods We estimated the dual-phase enhanced CT findings of 258 adrenal masses (42 ganglioneuromas, 216 lipid-poor adenomas) in 258 patients from July 2008 to July 2020 with ganglioneuromas and July 2016 to July 2020 with lipid-poor adenomas. The CT features between ganglioneuromas and lipid-poor adenomas were compared using independent two-sample t test, Mann–Whitney test, and ROC analysis.

Results Significant differences were detected in CT value of unenhanced (CT_U), CT value of arterial phase (CT_A), CT value of venous phase (CT_V), degree of enhancement in arterial phase, degree of enhancement in portal venous phase, age, tumor size [longest dimension, shortest dimension, mean dimension], shape, calcification between the ganglioneuroma and lipid-poor adenoma groups ($P < 0.05$). The results of receiver operating characteristics (ROC) analyses showed that areas under ROC curves of CT_U , CT_A and CT_V were 0.713, 0.878, and 0.914, respectively. When the cut-off values were set at 22.5 HU, 51.5 HU, and 53.5 HU for CT_U , CT_A , and CT_V , respectively, the three parameters had a sensitivity of 46.8%, 67.6%, and 88.0% and a specificity of 100%, 100%, and 88.1% in distinguishing ganglioneuromas from lipid-poor adenomas.

Conclusions Dual-phase enhanced abdominal CT can exhibit some of the primary imaging characteristics of ganglioneuromas and lipid-poor adenomas used to distinguish between these two entities.

Keywords Adrenal ganglioneuroma, Adrenal lipid-poor adenomas, Computed tomography, Adrenal tumor, ROC analysis

[†]Huajun Yu and Jian Wang contributed equally to this work.

*Correspondence:

Meihua Shao

shaomeihua2010@yeah.net

Full list of author information is available at the end of the article

Background

Adrenal masses are often detected incidentally in patients who undergoes routine abdominal computed tomography (CT) examinations. The discovery rate of adrenal mass lesions in the original population varied from 0.35 to 5% according to age [1]. Since a growing number of adrenal lesions are being detected, a better understanding of their imaging characteristics and their differential diagnosis is necessary [2]. Although the primary adrenal masses are nonfunctioning adrenal adenomas, potential differential diagnosis also exist including adrenal cysts, adrenal myelolipomas, adrenal ganglioneuromas [3–5]. In particular, when adrenal incidentalomas are detected, it is still a challenge for radiologists to distinguish adrenal ganglioneuromas from adrenal lipid-poor adenomas due to our rare knowledge of adrenal ganglioneuromas [6]. Although both adrenal ganglioneuromas and adrenal lipid-poor adenomas are benign and non-functional tumors, it is important to determine the lesions which require surgical intervention [7]. De Leo et al. [8] pointed out that one-third of adrenal adenomas may have a border line-malignant or malignant potential and deserve a specific follow-up protocol. While Dages et al. [9] showed that no recurrences or adrenal ganglioneuroma-specific mortality occurred during follow-up (range, 0–266 months).

The application of attenuation measurements on non-enhanced CT that assisting in distinguishing adrenal adenomas from nonadenomas has been reported by several studies [10, 11]. Most adenomas contain sufficient fat concentration, resulting in lower unenhanced CT value in adenomas compared with nonadenomas [12]. Adrenal lipid-poor adenomas are especially crucial because they could not be determined by unenhanced CT due to their relatively high attenuation, although they account for 10–40% of all adenomas [4, 13]. The value of delayed contrast-enhanced CT and MRI in differentiating adenomas from nonadenomas has been reported in previous reports [4, 14, 15]. However, delayed contrast-enhanced CT increased the exposure to radiation and the time–cost for patients, which have always been a major reason that limited their use. Previous researches have demonstrated the differential ability of dual-phase enhancement patterns between adrenal adenomas versus nonadenomas. Northcutt and Mohammed et al. [16, 17] showed dual-phase enhancement patterns could be used to differentiate adenoma and pheochromocytoma. Tu et al. [18] indicated that adrenal adenomas could be differentiated from adrenal metastases using single-phase contrast-enhanced CT.

To the best of our knowledge, few imaging characteristics of adrenal lipid-poor adenomas versus adrenal ganglioneuromas have been described in one study. In this

study, we focused on various quantitative parameters obtained from dual-phase enhanced abdominal CT that could be used to exclude adrenal ganglioneuromas from lipid-poor adenomas.

Methods

Patients

Our retrospective study obtained the agreement of institutional ethics review board of local hospital; the requirement for informed consent was waived. From July 2008 to July 2020 and July 2016 to July 2020, we searched consecutive records in the pathology and picture archiving and communication system (PACS) databases from local hospital for the diagnosis of adrenal ganglioneuromas and adenomas, respectively. Lipid-poor adenomas were defined as $CT_{U} \geq 10HU$ [13]. Finally, 42 ganglioneuromas and 216 lipid-poor adenomas were recruited based on the following inclusion criteria: (i) all subjects were confirmed by either abdominal operation or aspiration biopsy; (ii) both dual-phase contrast-enhanced CT images and clinical information were integrated; (iii) the CT examination were performed before the operation. The exclusion criteria included: (i) poor CT image quality; (ii) incomplete clinical data or dual-phase contrast-enhanced CT images. The subjects and exclusion criteria are shown in Fig. 1.

CT examinations

All CT scans were completed at 3–5 mm thickness based on the size of tumor by using one of the 4 CT scanners (SOMATOM Sensation 16, Siemens Healthcare, Forchheim, Germany; Siemens Definition AS 40/SOMATOM Definition Flash, Siemens Healthcare, Siemens Healthcare; LightSpeed VCT, GE Healthcare, Milwaukee, WI, USA). All the patients had both noncontrast CT and contrast-enhanced CT examinations. Contrast-enhanced images were obtained by intravenous injections with a total amount of 80–120 ml of contrast medium at a rate of 3–4 mL/s according to the patient's weight (1.0~1.5 ml/kg). Dual-phase enhanced CT scanning was performed after the onset of contrast injection was initiated at 30 s (arterial phase), and 60 s (portal phase), respectively.

CT image interpretation

The CT image interpretation was examined by two skilled radiologists, who had 10 and 15 years of experience in the diagnosis of abdominal diseases. The two radiologists scrutinized CT images in consensus at separate workplace by using blind method. CT observations were analyzed as follows: location, shape, number, CT value of unenhanced (CT_{U}), CT value of arterial phase (CT_{A}), CT value of venous phase (CT_{V}), degree of enhancement in

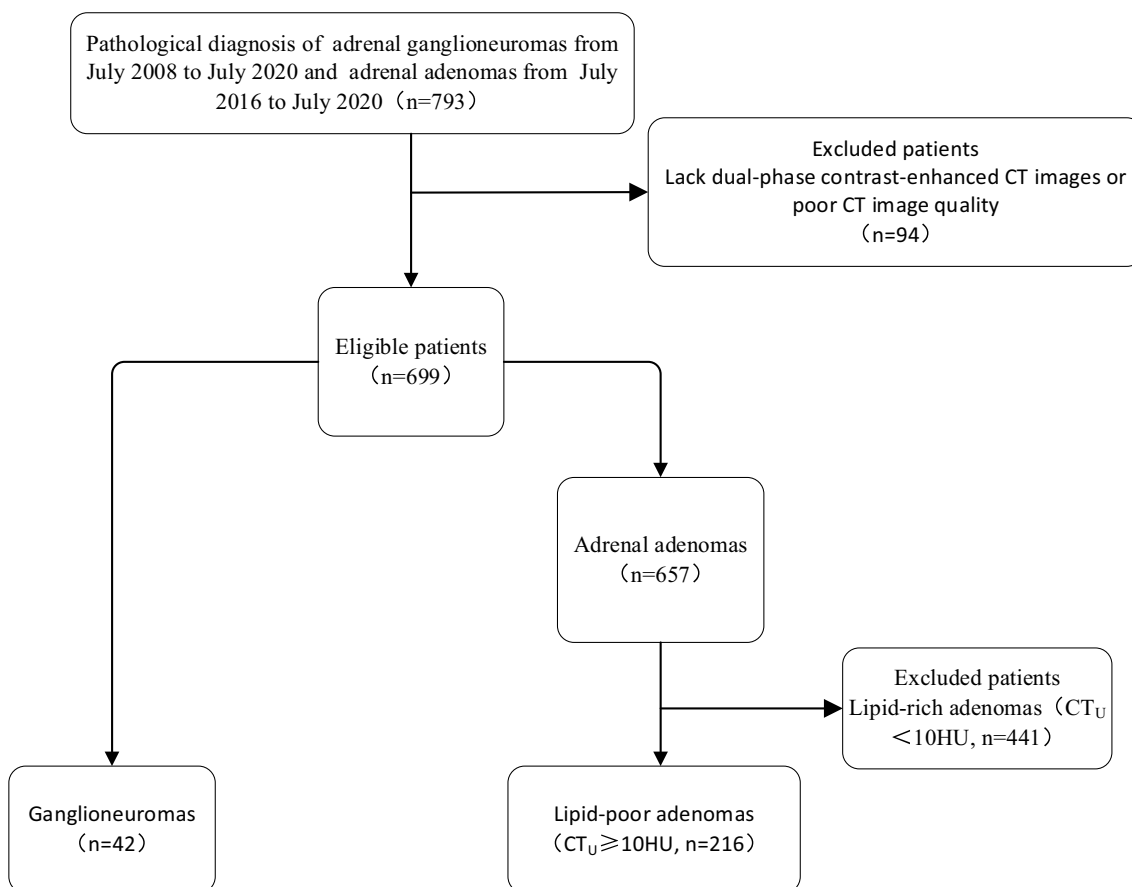


Fig. 1 The workflow for 258 patients who were eligible for participation in the research were selected from 793 patients who were confirmed by pathological diagnosis and finished dual-phase contrast-enhanced CT

arterial phase (DEAP), degree of enhancement in portal venous phase (DEPP), longest dimension (LD), shortest dimension (SD), shape, cystic degeneration, hemorrhage, and calcification. Cystic degeneration was defined as unenhanced portion with density ranging from -20 to 20 HU, and the presence of calcification with the density above 120 HU [19]. Furthermore, the longest dimension and shortest dimension of the lesion, where it appeared largest and shortest on the same axial images, were measured, respectively. Mean dimension (MD) referred to $(LD + SD)/2$. The clinical features and CT findings of the ganglioneuromas and lipid-poor adenomas were compared.

Statistical analysis

Statistical analysis were performed by SPSS 20.0 (SPSS, Inc; Chicago, Illinois). Shapiro–Wilk *W* test was performed to test the normality distribution of all continuous variables. Statistical differences between these two groups were analyzed by either independent two-sample *t* test or the Mann–Whitney test as appropriate. The

Chi-square or Fisher’s exact test was used for categorical variables. Each $P < 0.05$ was considered statistically significant.

Receiver operating characteristic curve (ROC) analysis was performed to calculate the diagnostic accuracy of CT_U , CT_A , CT_V , age, and tumor size for differentiating ganglioneuromas and lipid-poor adenomas. The sensitivity, specificity, area under the receiver operating characteristic curve (AUC) were calculated [20]. Subsequently, the best cutoff values were determined by ROC curve by maximizing the Youden index (Youden index = sensitivity + specificity – 1).

Results

Demographic characteristics

A detailed demographic data of adrenal masses are summarized in Table 1. The mean age of ganglioneuromas was 38.1 years ± 13.2 (range, 14–74 years) compared with 52.4 years ± 11.8 (range, 20–76 years) for lipid-poor adenomas ($P < 0.001$). There was no significant difference in gender between these two groups ($P \geq 0.05$).

Table 1 Demographic of 42 cases of adrenal ganglioneuromas and 216 cases of adrenal lipid-poor adenomas

| | ganglioneuromas | lipid-poor adenomas | P value |
|--------------------|-----------------|---------------------|---------|
| Number of patients | 42 | 216 | / |
| Age±SD | 38.1±13.2 | 52.4±11.80 | 0.000 |
| Male/female ratio | 20/22 | 78/138 | 0.160 |

CT findings analysis

Comparisons of ganglioneuromas and lipid-poor adenomas are presented in Table 2. The mean CT_U, CT_A, and CT_V of ganglioneuromas were 32.3 HU±5.2, 37.0

HU±7.1, and 44.7 HU±10.1 compared with 25.3 HU±10.1, 66.4 HU±26.4, and 76.3 HU±26.4 for the lipid-poor adenomas, respectively (P<0.001) (Figs. 2, 3 and 4). The 42 ganglioneuromas had a mean DEAP, and DEPP of 4.7 HU±5.2, and 12.4 HU±9.3 compared with 41.1 HU±22.2, and 51.0 HU±20.2 for the 216 lipid-poor adenomas, respectively (P<0.001). The mean diameter of ganglioneuromas was 34.9 mm±19.7 (range, 15–112 mm) compared with 21.3 mm±9.3 (range, 8–67 mm) for lipid-poor adenomas (P<0.05).

No significant difference was found in location between ganglioneuromas and lipid-poor adenomas (P≥0.05). The shape of tumors was significantly different between

Table 2 CT findings of 42 cases of adrenal ganglioneuromas and 216 cases of lipid-poor adenomas

| | Ganglioneuromas | Lipid-poor adenomas | P value |
|------------------------------|-----------------|---------------------|--------------|
| Number of patients | 42 | 216 | / |
| CT value (HU) | | | |
| CT _U | 32.3±5.2 | 25.3±10.1 | 0.000 |
| CT _A | 37.0±7.1 | 66.4±26.4 | 0.000 |
| CT _V | 44.7±10.1 | 76.3±23.3 | 0.000 |
| DEAP | 4.7±5.2 | 41.1±22.2 | 0.000 |
| DEPP | 12.4±9.3 | 51.0±20.2 | 0.000 |
| LD (mm) | 40.1±22.3 | 23.6±10.3 | 0.000 |
| SD (mm) | 29.7±17.7 | 18.9±8.6 | 0.000 |
| Mean D (mm) | 34.9±19.7 | 21.3±9.3 | 0.000 |
| Shape | | | 0.000 |
| Location (right: left gland) | 24/18 | 102/114 | 0.239 |
| Round | 5 | 95 | |
| Oval | 22 | 131 | |
| Irregular | 15 | 32 | |
| Cystic degeneration | 1 | 22 | 0.104 |
| Hemorrhage | 1 | 3 | 0.634 |
| Calcification | 10 | 13 | 0.001 |

CT_UCT value of unenhanced, CT_ACT value of arterial phase, CT_VCT value of venous phase, DEAPDegree of enhancement in arterial phase, DEPPDegree of enhancement in portal venous phase, LDLongest dimension, SDShortest dimension, Mean D Mean dimension

P values written in bold indicate a significant difference between the lesions

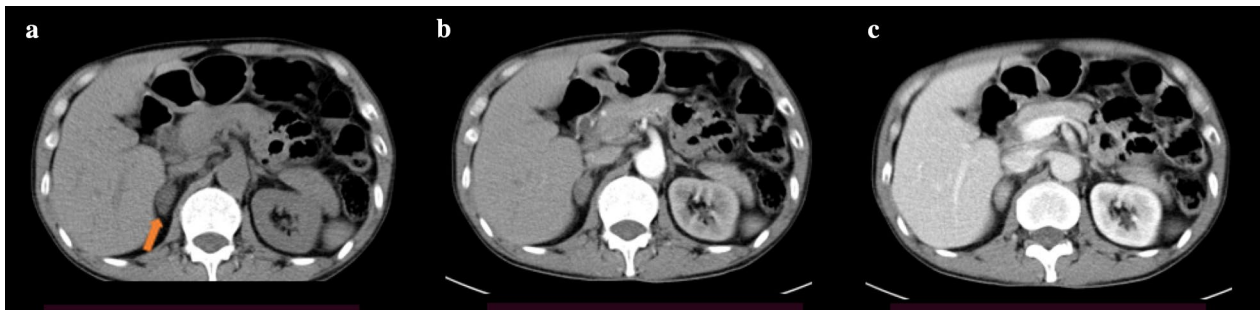


Fig. 2 A surgery-proven ganglioneuromas in a 42-year-old patient. **a** Unenhanced CT image showed a round-shaped nodule with a mean size of 15 mm from right adrenal (arrow). The CT value of unenhanced was 38 HU. **b, c** Enhanced CT images depicted that the CT value of arterial phase, and venous phase was 42, and 47 HU, respectively



Fig. 3 A surgery-proven lipid-poor adenomas. 43-year-old male patient examined by abdominal CT for incidental finding. **a** Unenhanced CT image depicted an oval-shaped nodule with a mean size of 19 mm from right adrenal (arrow). The CT value of unenhanced was 24 HU. **b, c** Enhanced CT images showed that the nodule manifested as homogenous enhancement with CT value of arterial phase, and venous phase was 51, and 89 HU, respectively

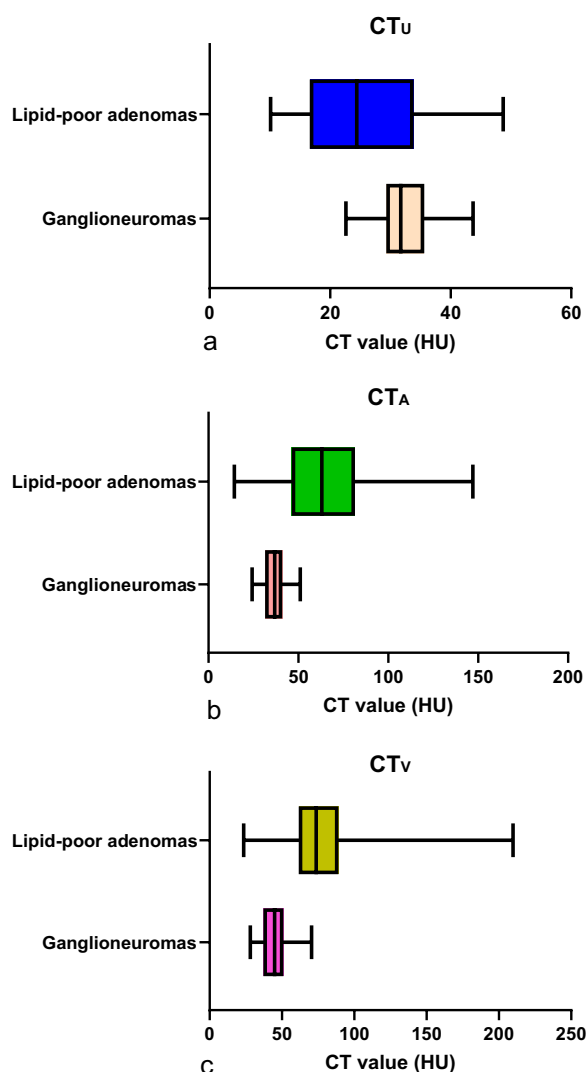


Fig. 4 Box illustrates the attenuation value of unenhanced (a), arterial phase (b), and venous phase (c) of ganglioneuromas and lipid-poor adenomas

ganglioneuromas and lipid-poor adenomas ($P < 0.001$). Besides, the detection rate of calcification was significantly different for these two groups ($P < 0.05$). The presence of cystic degeneration, hemorrhage were not significant between ganglioneuromas and lipid-poor adenomas ($P \geq 0.05$). The results of ROC curve analysis depicted that AUC of CT_U, CT_A and CT_V were 0.713, 0.878, and 0.914, respectively. When the cut-off points were set at 22.5 HU, 51.5 HU, and 53.5 HU for CT_U, CT_A, and CT_V, respectively, the three parameters had a sensitivity of 46.8%, 67.6%, and 88.0% and a specificity of 100%, 100%, and 88.1% in distinguishing between ganglioneuromas and lipid-poor adenomas. Sensitivity, specificity for distinguishing ganglioneuromas and lipid-poor adenomas using a cut-off age of 50.5 years were 63.4%, 85.7%, respectively; using the mean diameter threshold of 28.3 mm, they were 45.2%, 93.1%, respectively (Table 3, Fig. 5).

Discussion

As far as we know, the present report represents the first report to distinguish adrenal ganglioneuromas from lipid-poor adenomas using dual-phase enhanced CT scan as described. With the increased use of abdominal CT-scans, incidental detection of adrenal tumor is becoming more often. It is vital to discriminate adrenal ganglioneuromas from adenomas, particularly in the presence of a lipid-poor adrenal tumor. This retrospective study focused on several CT quantifiable parameters obtained from the unenhanced and dual-phase enhanced CT for differentiation of adrenal ganglioneuromas from lipid-poor adenomas. Our results manifested that CT value (CT_U, CT_A, CT_V, DEAP, DEPP), age, tumor diameter, shape, and calcification were significant differently between the adrenal ganglioneuromas and lipid-poor adenomas.

Table 3 Diagnostic performance of CT values, age, and mean diameter for ganglioneuromas vs lipid-poor adenomas

| | AUC | 95% CI | Cut-off value (%) | Sensitivity% | Specificity% | P value |
|-----------------|-------|-------------|-------------------|--------------|--------------|---------|
| CT _U | 0.713 | 0.650~0.775 | ≤ 22.5 HU | 46.8 | 100 | 0.000 |
| CT _A | 0.878 | 0.836~0.920 | ≥ 51.5 HU | 67.6 | 100 | 0.000 |
| CT _V | 0.914 | 0.876~0.952 | ≥ 53.5 HU | 88.0 | 88.1 | 0.000 |
| Age | 0.798 | 0.605~0.821 | ≥ 50.5 years | 63.4 | 85.7 | 0.000 |
| Mean D | 0.758 | 0.679~0.837 | ≤ 28.3 mm | 45.2 | 93.1 | 0.000 |

Forty-two adrenal ganglioneuromas and 216 lipid-poor adenomas were evaluated. The criterion value was determined by the maximum value of Youden's index (sensitivity + specificity - 1)

AUC Area under the receiver operating characteristic curve, CT_UCT value of unenhanced, CT_ACT value of arterial phase, CT_VCT value of venous phase, Mean D Mean dimension

In our study, we found that ganglioneuromas had a higher CT_U than lipid-poor adenomas ($P < 0.001$), but a large overlap occurred between these 2 entities. Lee, Miyake et al. pointed out that the threshold of 15–25 HU on noncontrast CT was a cut-off for discrimination between adenomas and nonadenomas [21, 22]. The CT_U criterion yielded 100% specificity, but the sensitivity of 46.8% was not high to become a discriminator. For our enhanced CT parameters, the CT_A and CT_V of lipid-poor adenomas were significantly higher than that of the ganglioneuromas. ($P < 0.001$). The threshold value of 51.5 HU of CT_A, and 53.5 HU of CT_V, respectively, yielded 67.6%, and 88.0% sensitivity and 100%, and 88.1% specificity for discrimination between ganglioneuromas and lipid-poor adenomas. Results from prior reports indicate that the mean enhanced CT value of the lipid-poor adenomas ranged from 55 to 83 HU [4, 13, 23]. Besides, the accessory quantitative parameters such as DEAP and DEPP were also significantly different between lipid-poor adenomas and ganglioneuromas which were obtained from dual-phase enhanced CT. Previous reports have confirmed that absolute or relative percentage washout

of contrast material obtained from delayed contrast-enhanced CT scans (5 min, 10 min, 15 min, 30 min) is a useful method for the differentiation of lipid-poor from adrenal nonadenomas which reached a relatively high sensitivity and specificity [4, 24]. However, the high diagnostic efficiency was at the expense of long time of CT scan which also means more radiation dose for patients. Hence, our results suggested that CT attenuation value from early contrast CT could achieve considerable diagnostic efficiency for the differentiation between adrenal ganglioneuromas from lipid-poor adenomas compared with delayed contrast CT, which had vital clinical application value.

Adrenal lipid-poor adenomas were 14 years older, ranging from 20 to 76 years (mean, 52.4 years), than adrenal ganglioneuromas that ranged from 14 to 74 years (mean, 38.1 years) ($P < 0.001$). A prior study addressed that the discovery rate of adrenal adenomas increases with age [25]. Our results showed that the mean age of lipid-poor adenomas were older than 50 years which were similar to previous reports, whereas precedent case reports on adrenal ganglioneuromas viewed that they

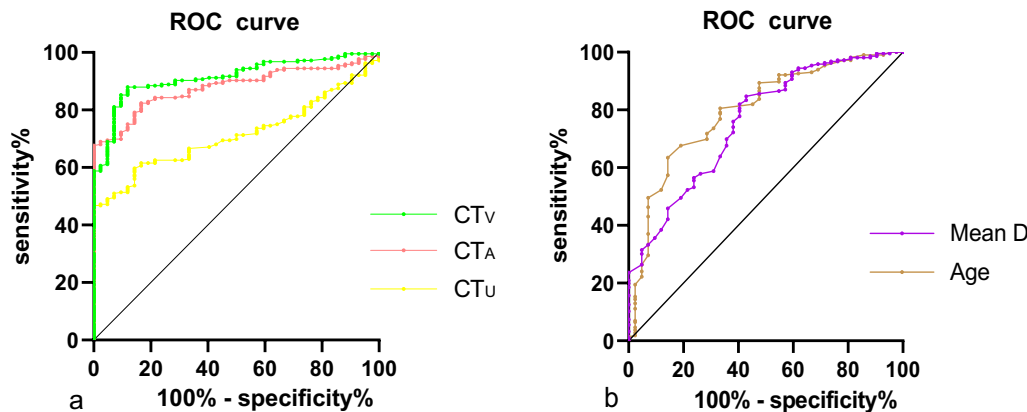


Fig. 5 ROC curves of CT value (a), mean size (b), and age (b) for the diagnosis of adrenal ganglioneuromas. Areas under ROC curve of CT_U, CT_A, CT_V, mean size, and age are 0.713, 0.878, 0.914, 0.758, and 0.798, respectively

mostly occur in older children and young which were not consist with our findings [4, 23, 26]. However, our results showed that age did not have a high diagnostic effectiveness in distinguishing lipid-poor adenomas from adrenal ganglioneuromas with a sensitivity and specificity of 63.4% and 85.7%, respectively, when the cut-off was set at 50.5 years old. Consequently, our analysis suggested that age may not be a useful discriminatory factor for distinguishing adrenal ganglioneuromas from adrenal lipid-poor adenomas.

The mean size of adrenal ganglioneuromas was 14 mm larger than lipid-poor adenomas ($P < 0.05$). Nevertheless, prior studies have reported overlap in size between adenomas and nonadenomas, which was also noticeable in this study [24, 27, 28]. The size criterion yielded 93.1% specificity, but the sensitivity of 45.2% was not high to be acknowledged as a discriminator.

Our results showed that most ganglioneuromas (88.1% [37 of 42]) were of oval or irregular shape, but lipid-poor adenomas (85.2% [184 of 216]) were more likely to have a round or oval shape ($P < 0.05$). In general, round, oval shapes are considered as a feature of benign tumor, while the irregular contour is associated with malignant lesions [29]. Although the difference of shape between ganglioneuromas and adenomas is significant, it is not infallible as criterion in discriminating between ganglioneuromas and adenomas due to the fact that there is considerable overlap in shape. In our study, both cystic degeneration and hemorrhage were not likely to occur in ganglioneuromas and adenomas. It has been reported that cystic degeneration and hemorrhage typically occurs in adenomas when the size was larger than 4 cm [30].

The described calcification discovery rate ranged from 30 to 60% in ganglioneuromas, whereas only small cases have reported the presence of calcifications in adenomas [31–33]. In our study, the detection rate of calcification was 23.8% (10 of 42) in ganglioneuromas, compared with 6.0% (13 of 216) for lipid-poor adenomas ($P < 0.05$). Hence, we speculated that the presence of calcifications was more conducive to the diagnosis of ganglioneuromas.

Our study had several limitations. First, the number of ganglioneuromas was relatively smaller than that of lipid-poor adenomas due to its rarity. As a result of the small number of included patients of adrenal ganglioneuromas, larger, multicentric trials are required to confirm these results. Second, our study had the connatural disadvantages of retrospective analysis, such as detection, selection, and confounding biases. The adrenal adenomas and ganglioneuromas enrolled in this study were obtained from two hospitals; however, complete clinical and CT data could not be acquired for all samples. Hence, the potential selection bias and confounding bias was inevitable. Besides, our data were obtained by using different

CT devices which probably have minor effect to the final results. However, we insist that our data exploited beneficial information related to ganglioneuromas and lipid-poor adenomas. Finally, we did not compare absolute percentage washout ratio (APW) and relative percentage washout ratio (RPW) between these two groups whose diagnostic values have been confirmed in the discrimination of adenomas versus nonadenomas. For further studies, a larger number of adrenal ganglioneuromas cases are necessary. Moreover, CT scans should be uniformed to conform the differential ability of dual-phase enhanced CT in these two entities.

Conclusions

In conclusion, enhanced CT of the abdomen could be a suitable approach for distinguishing ganglioneuromas from lipid-poor adenomas.

Abbreviations

| | |
|-----------------|--|
| CT | Computerized tomography |
| CT _U | CT value of unenhanced |
| CT _A | CT value of arterial phase |
| CT _V | CT value of venous phase |
| DEAP | Degree of enhancement in arterial phase |
| DEPP | Degree of enhancement in portal venous phase |
| LD | Longest dimension |
| SD | Shortest dimension |
| MD | Mean dimension |
| PACS | Picture archiving and communication system |
| ROC | Receiver operating characteristic curve |
| AUC | Area under the receiver operating characteristic curve |
| APW | Absolute percentage washout ratio |
| RPW | Relative percentage washout ratio |

Acknowledgements

Not applicable.

Author contributions

Guarantor of integrity of the entire study was HJY and JW. Study concepts and design were contributed by HJY, ZFN, JW, and MHS. Literature research was contributed by HJY, ZFN, JW, and MHS. Clinical studies were contributed by HJY, ZFN, and JW. Data analysis was contributed by HJY and JW. Statistical analysis was contributed by HJY and JW. Manuscript editing was contributed by MHS. All authors have read and approved the manuscript.

Funding

No funding was obtained for this study.

Availability of data and materials

All data analyzed during this research are included in this published article.

Declarations

Ethics approval and consent to participate

This retrospective study was approved by the Institutional Review Board and Ethics Committee of Tongde Hospital of Zhejiang Province, Hangzhou, Zhejiang Province, China (no KTSC2017004), and the requirement for informed consent was waived.

Consent for publication

Not applicable.

Competing interests

The authors declare no conflict of interest.

Author details

¹Department of Radiology, Affiliated Zhejiang Hospital, Zhejiang University School of Medicine, Hangzhou 310013, Zhejiang Province, China. ²Department of Radiology, Tongde Hospital of Zhejiang Province, No. 234, Gucui Road, Hangzhou 310012, Zhejiang Province, China. ³Department of Radiology, Sir Run Run Shaw Hospital of Zhejiang University School of Medicine, Hangzhou 310016, Zhejiang Province, China.

Received: 1 August 2023 Accepted: 15 October 2023

Published online: 24 October 2023

References

- Xu Y, Wang Z, Bi Y et al (2018) Correlation between CT features of adrenocortical and adrenal medullary tumors and expression of miR-96 in serum. *Oncol Lett* 16(2):2053–2057. <https://doi.org/10.3892/ol.2018.8863>
- Mosconi C, Vicennati V, Papadopoulos D et al (2017). Can Imaging Predict Subclinical Cortisol Secretion in Patients With Adrenal Adenomas? A CT Predictive Score. *AJR Am J Roentgenol* 209(1):122–129. <https://doi.org/10.2214/AJR.16.16965>
- Liu T, Sun H, Zhang H et al (2018) Distinguishing adrenal adenomas from non-adenomas with multidetector CT: evaluation of percentage washout values at a short time delay triphasic enhanced CT. *Br J Radiol* 92(1094):20180429
- Kebapci M, Kaya T, Gurbuz E et al (2003) Differentiation of adrenal adenomas (lipid rich and lipid poor) from nonadenomas by use of washout characteristics on delayed enhanced CT. *Abdom Imaging* 28(5):709–15. <https://doi.org/10.1007/s00261-003-0015-0>
- Lee JH, Chai YJ, Kim TH et al (2016) Clinicopathological features of ganglioneuroma originating from the adrenal glands. *World J Surg* 40:2970–2975
- Adas M, Koc B, Adas G et al (2014) Ganglioneuroma presenting as an adrenal incidentaloma: a case report. *J Med Case Rep* 8:131. <https://doi.org/10.1186/1752-1947-8-131>
- Taffel M, Haji-Momenian S, Nikolaidis P et al (2012) Adrenal imaging: a comprehensive review. *Radiol Clin N Am* 50(2):219–43
- De Leo A, Mosconi C, Zavatta G et al (2020) Radiologically defined lipid-poor adrenal adenomas: histopathological characteristics. *J Endocrinol Invest* 43(9):1197–1204
- Dages KN, Kohlenberg JD, Young WF Jr et al (2021) Presentation and outcomes of adrenal ganglioneuromas: a cohort study and a systematic review of literature. *Clin Endocrinol (Oxf)* 95(1):47–57
- Ying WU, Han Z, Zhu M et al (2017) The diagnostic value of minimum attenuation values in lipid-poor adenomas on unenhanced CT. *J Med Imaging* 027(9):1738–1741, 1756
- Mz A, Jq B, Zh C (2016) Evaluate the efficacy of minimum attenuation value in differentiation of adrenal adenomas from nonadenomas on unenhanced CT. *Clin Imaging* 40(1):86–89
- Al-Thani H, El-Menyar A, Al-Sulaiti M et al (2015) Adrenal mass in patients who underwent abdominal computed tomography examination. *N Am J Med Sci* 7(5):212–219
- Kamiyama T, Fukukura Y, Yoneyama T et al (2009) Distinguishing adrenal adenomas from nonadenomas: combined use of diagnostic parameters of unenhanced and short 5-minute dynamic enhanced CT protocol. *Radiology* 250(2):474–81. <https://doi.org/10.1148/radiol.2502080302>
- Halefoglu AM, Bas N, Yasar A et al (2010) Differentiation of adrenal adenomas from nonadenomas using CT histogram analysis method: a prospective study. *Eur J Radiol* 73(3):643–651. <https://doi.org/10.1016/j.ejrad.2008.12.010>
- Siegelman ES (2000) MR imaging of the adrenal neoplasms. *Magn Reson Imaging Clin N Am* 8(4):769–786
- Northcutt BG, Raman SP, Long C et al (2013) MDCT of adrenal masses: can dual-phase enhancement patterns be used to differentiate adenoma and pheochromocytoma. *AJR Am J Roentgenol* 201(4):834–839
- Mohammed MF, ElBanna KY, Ferguson D et al (2018) Pheochromocytoma versus adenoma: role of venous phase CT enhancement. *AJR Am J Roentgenol* 210(5):1073–1078
- Tu W, Verma R, Krishna S et al (2018) Can adrenal adenomas be differentiated from adrenal metastases at single-phase contrast-enhanced CT. *AJR Am J Roentgenol* 211(5):1044–1050
- Ctvrtilik F, Herman M, Student V et al (2009) Differential diagnosis of incidentally detected adrenal masses revealed on routine abdominal CT. *Eur J Radiol* 69:243–252
- Meng X, Chen X, Shen Y et al (2017) Proton-density fat fraction measurement: a viable quantitative biomarker for differentiating adrenal adenomas from nonadenomas. *Eur J Radiol* 86:112–118. <https://doi.org/10.1016/j.ejrad.2016.11.001>
- Miyake H, Takaki H, Matsumoto S et al (1995) Adrenal nonhyperfunctioning adenoma and nonadenoma: CT attenuation value as discriminative index. *Abdom Imaging* 20(6):559–62. <https://doi.org/10.1007/BF01256711>
- Park SH, Kim MJ, Kim JH et al (2007) Differentiation of adrenal adenoma and nonadenoma in unenhanced CT: new optimal threshold value and the usefulness of size criteria for differentiation. *Korean J Radiol* 8(4):328–335
- Caoili EM, Korobkin M, Francis IR et al (2000) Delayed enhanced CT of lipid-poor adrenal adenomas. *AJR Am J Roentgenol* 175(5):1411–1415. <https://doi.org/10.2214/ajr.175.5.1751411>
- Caoili EM, Korobkin M, Francis IR et al (2002) Adrenal masses: characterization with combined unenhanced and delayed enhanced CT. *Radiology* 222:629–633
- Young WF (2007) The incidentally discovered adrenal mass. *N Engl J Med* 356:601–610
- Qing Y, Bin X, Jian W et al (2010) Adrenal ganglioneuromas: a 10-year experience in a Chinese population. *Surgery* 147:854–860
- Caoili EM, Korobkin M, Francis IR et al (2000) Delayed enhanced CT of lipid-poor adrenal adenomas. *AJR Am J Roentgenol* 175:1411–1415
- Peña CS, Boland GW, Hahn PF et al (2000) Characterization of indeterminate (lipid-poor) adrenal masses: use of washout characteristics at contrast-enhanced CT. *Radiology* 217:798–802
- Jia AH, Du HQ, Fan MH et al (2015) Clinical and pathological analysis of 116 cases of adult adrenal cortical adenoma and literature review. *Oncotargets Ther.* 8:1251–7. <https://doi.org/10.2147/OTT.S81831>
- Newhouse JH, Heffess CS, Wagner BJ et al (1999) Large degenerated adrenal adenomas: radiologic-pathologic correlation. *Radiology* 210:385–391
- Paster SB, Rosen RT (1974) Calcification in benign adrenal adenoma. *Urology* 3:646–648
- Linos D, Tsirlis T, Kapralou A et al (2011) Adrenal ganglioneuromas: incidentalomas with misleading clinical and imaging features. *Surgery* 149:99–105
- Rondeau G, Nolet S, Latour M et al (2010) Clinical and biochemical features of seven adult adrenal ganglioneuromas. *J Clin Endocrinol Metab* 95:3118–3125

Publisher's Note

Springer Nature remains neutral with regard to jurisdictional claims in published maps and institutional affiliations.

Submit your manuscript to a SpringerOpen[®] journal and benefit from:

- Convenient online submission
- Rigorous peer review
- Open access: articles freely available online
- High visibility within the field
- Retaining the copyright to your article

Submit your next manuscript at ► [springeropen.com](https://www.springeropen.com)